

Prediction of the Ferrite Layer Microstructure during Decarburization

Koutarou HAYASHI*

Toshinobu NISHIBATA

Abstract

In order to examine the rate-controlling process of the decarburization behavior in the Fe-0.87 at% C alloy, the growth behavior of the ferrite layer was analyzed. According to the isothermal annealing experiments, the alloy possessed the ferrite and cementite two phase microstructures at 953 K and the ferrite and austenite two phase microstructures at the temperature range between 993 K to 1073 K. Austenite single phase microstructure was formed above 1153 K. However, the ferrite layer appeared on the surface of the alloy below 1153 K due to decarburization. The formation of the ferrite layer can be predicted by the calculation of phase equilibria in the binary Fe-C system. Moreover, the parabolic coefficient of the growth for the ferrite layer is calculated by a moving boundary model based on the diffusion of C in the layer. The calculated values are almost equal to those of the measured parabolic coefficient by the isothermal annealing experiments.

1. Introduction

High-strength steel contains various alloy elements such as Si and Mn in addition to approximately 1.0 at% C. To increase the strength of the carbon steel, it is often quenched after heating to a temperature higher than A_{c3} .¹⁾ As the temperature rises during heating, the chemical reactions of C in steel with scale, vapor, or other components of the atmosphere are accelerated. When carbon steel is heated, therefore, carbon concentration sometimes decreases at and near the surface;²⁾ this phenomenon is referred to as decarburization. The strength and other mechanical properties of steel are affected by decarburization.^{3,4)} The effect is pronounced especially when a structure containing ferrite (α) in large amounts or a single-phase structure of α forms at the surface.⁵⁾ The expression “ferrite layer(s)” hereinafter refers to such a single-phase structure of α forming at the surface.

There have been many experimental studies on the structural change of carbon steel due to decarburization and the growth rate of the ferrite layer.⁶⁻¹⁷⁾ When carbon steel is decarburized in the temperature range in which both α and austenite (γ) can exist in an equilibrium, a ferrite layer forms at the surface and grows continuously inside, and the growth rate is largest in the temperature range from 1023 to 1073 K.^{9, 12, 16, 17)} The growth rate of the ferrite layer being affected by temperature and also the steel chemical composition

demonstrates that decarburization is a complicated phenomenon. For example, when the steel contains elements such as Si and P, the growth is accelerated, and when it contains Ni, Cr, Mn, etc., it is slowed down.^{9, 12)} To understand decarburization of carbon steel, therefore, it is necessary to clarify the effects of alloying elements over the formation of the above structures based on experiments of the Fe-C binary system. Nevertheless, there have been few reports on the decarburization reactions of the binary system.¹²⁾

In polycrystalline materials, grain boundaries can serve as the routes for fast diffusion of component elements.¹⁸⁾ In the study of structural change during heating, therefore, it is essential to consider the effects of the grain-boundary diffusion of solutes and their volume diffusion. It has been reported regarding diffusion and the subsequent reactions of dissimilar metal elements that both grain-boundary diffusion and volume diffusion contribute to the growth of the ferrite layer.^{19, 20)} For this reason, to clarify the rate-determining process for decarburization reactions, it is necessary to analyze the growth of the ferrite layer and the α grain growth in the layer. However, there have been only a limited number of experimental studies into the grain growth of steel accompanied by decarburization,²¹⁾ and the grain growth in ferrite layers is unclear.

Considering this situation, we conducted the following tests. Cold-rolled sheets of an Fe-0.87 at% C alloy were isothermally an-

* Senior Researcher, PhD in Engineering, Sheet & Coil Research Lab., Steel Research Laboratories
20-1 Shintomi, Futtsu City, Chiba Pref. 293-8511

nealed in a decarburizing atmosphere at different temperatures from 953 to 1193 K. The growth of the ferrite layer forming as a result and the growth of α grains in the layer were examined through microscope observation, and the rate-determining process of decarburization reactions was identified based on the results. In addition, assuming that the volume diffusion of C atoms determines the rate of decarburization reactions, the structure of the ferrite layer during heating was predicted using a moving boundary model that takes thermodynamics and diffusion kinetics into consideration, and the prediction result was compared with the result of the isothermal annealing. The present paper reports the results of these tests.

2. Body

2.1 Test method

Table 1 shows the chemical composition of the steel used. Si, Mn, P, S, Al, and N are impurities, and the specimen steel is substantially a binary alloy of Fe and C; it is hereinafter referred to as the Fe-0.87 at% C alloy. The alloy was melted in a vacuum melting furnace, cast into ingots 17 kg in weight, heated at 1473 K for 3600 s, forged at 1223 K or higher, and then air cooled to room temperature. The forged ingots were machined into slabs, 20 mm thick, 160 mm wide, and 100 mm long each, the slabs were heated at 1523 K for 1800 s, and hot rolled at 1123 K or higher into hot-rolled sheets 5 mm thick. The hot-rolled sheets were cooled to 923 K at a rate of 50 K/s, held at the temperature for 1800 s, and then cooled to room temperature at a rate of 5.6×10^{-3} K/s. The hot-rolled sheets were machined at the top and bottom surfaces to a depth of 0.75 mm to remove the scale, and then cold rolled to a thickness of 1.2 mm.

The cold-rolled sheets thus prepared were heated at a rate of 10 K/s to different temperatures, isothermally annealed at those temperatures for 0 to 1600 s, and specimens for structural observation were prepared. The temperature of annealing ranged from 953 to 1193 K, the atmosphere consisted of 2 vol% hydrogen and 98 vol% nitrogen, the dew point was 268 K, and the sheets were cooled to room temperature at a rate of 10 K/s. Separately from the above, the Ac_1 and Ac_3 of the Fe-0.87 at% C alloy were determined by heating

some of the cold-rolled sheets to 1273 K at a rate of 10 K/s. The specimens for microscopic observation were cut out from hot-rolled sheets, cold-rolled sheets, and cold-rolled-and-annealed (at different temperatures) sheets, buffed with alumina, and etched with nital at a section parallel to the rolling direction, and observed through an optical microscope or a laser microscope. The phases thus observed at the section were identified by X-ray diffractometry (XRD). The carbon concentration distribution at the section was measured using an electron probe micro analyzer (EPMA); for this measurement, a calibration curve was drawn using carbon steel of a known chemical composition as a reference.

2.2 Growth of ferrite layer

Figure 1 shows a sectional photomicrograph of the hot-rolled specimen taken through an optical microscope; the structure consisted of ferrite (α) and cementite (θ). The α phase was mostly in the form of allotriomorph, and some part was acicular. The grain diameter of the ferrite was calculated at 20 μm by the quadrature method.²²⁾ The θ phase was in grains, which were distributed mainly at the grain boundaries of α .

Figure 2 shows sectional microstructures of the cold-rolled sheets of the Fe-0.87 at% C alloy isothermally annealed for 600 s at different temperatures from 953 to 1193 K; they were passed through a laser microscope. The Ac_1 and Ac_3 were 1014 and 1142 K, respectively. As seen in Fig. 2(a), the specimen annealed at 953

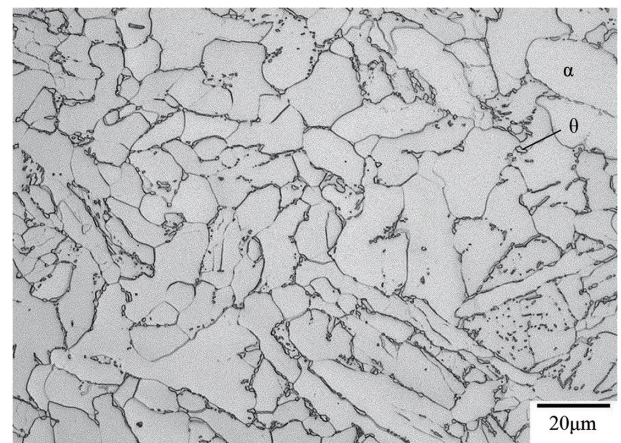


Fig. 1 Microstructure of the hot-rolled Fe-0.87 at% C alloy

Table 1 Chemical composition of the steel investigated (at%)

C	Si	Mn	P	S	N	Fe
0.87	0.01	0.01	0.01	0.001	0.006	Bal.

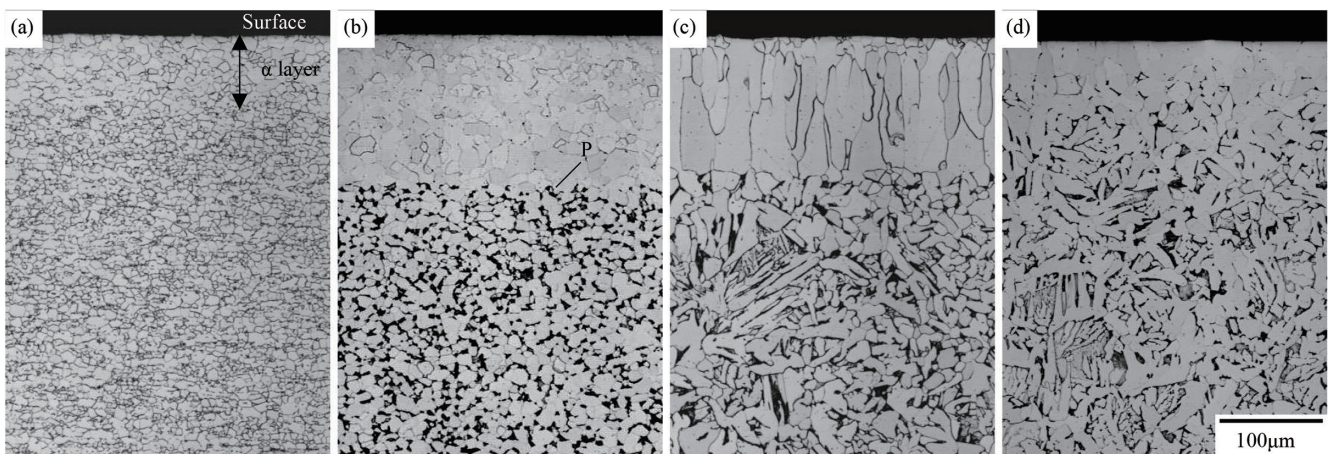


Fig. 2 Cross-sectional microstructures of Fe-0.87 at% C alloy annealed for 600 s at (a) 953 K, (b) 1033 K, (c) 1153 K and (d) 1193 K

K had a recrystallized dual-phase structure of α and θ . At 1033 K, however, the γ phase formed, and the structure was a dual-phase structure of α and γ . The bright areas in Fig. 2(b) are α , and the dark areas are pearlite (P), which formed from the γ phase during the cooling after the annealing.

When the annealing temperature was 1142 K or higher, in contrast, the specimen sheets consisted of a single-phase structure of γ . As seen in Fig. 2(c) and (d), γ transforms into a dual phase of acicular ferrite and P or a single-phase of bainite. As seen in parts (a), (b), and (c), the structure at and near the surface and that in the interior were different, with a distinct boundary between them, and the former was a layered structure of α . The structure of the surface layer was identified through the XRD method to be a single-phase structure of α . It has thus been made clear that ferrite forms in the surface layer when sheets of an Fe-0.87 at% C alloy are isothermally annealed at temperatures from 953 to 1153 K. The thickness of the ferrite surface layer at an annealing temperature of 1033 K was roughly 150 μm .

A ferrite surface layer was found also in the specimen of Fig. 2 (d), but the boundary between it and the structure of γ in the interior was not as clear. This is because in this specimen, which was annealed at 1193 K, the C concentration in γ decreased in the surface layer, and this γ of a low C concentration transformed into α during cooling to form the ferrite layer, which means that the ferrite layer did not form during the isothermal annealing at 1193 K. Note that, as will be explained later, such ferrite formation at different temperatures can be predicted based on the phase diagram of the Fe-C binary system.^{11, 23)}

Carbon concentration was measured with an EPMA at the section shown in Fig. 2(b). **Figure 3** shows a carbon concentration profile in the direction perpendicular to the sheet surface; here, the ordinate represents C concentration and the abscissa the distance from the sheet surface. It is clear from the graph that the concentration profile was different at different sides of the boundary between the surface and the inside structures: while the C concentration was low in the ferrite surface layer, it was uneven and locally high in the

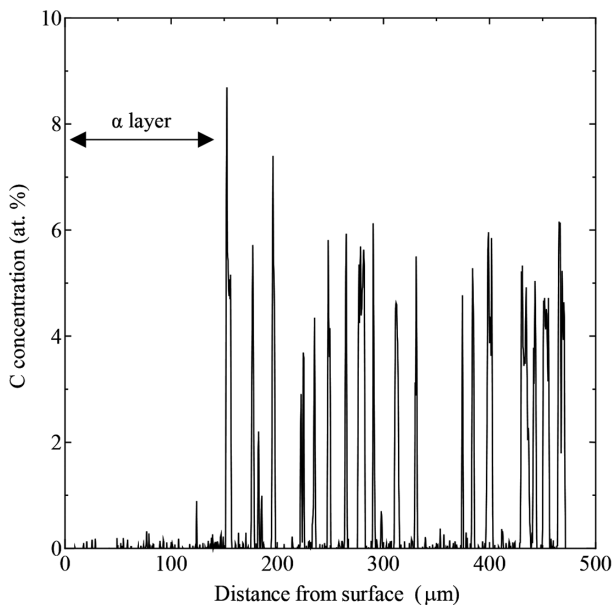


Fig. 3 Carbon concentration profile of Fe-0.87 at% C alloy annealed for 600 s at 1033 K

inside structure consisting of α and P. In other words, the C concentration in the ferrite layer was lower than the average in the specimen interior, which evidenced decarburization at and near the surface. This indicates that an Fe-0.87 at% C alloy is decarburized during isothermal annealing at temperature from 953 to 1153 K, a ferrite layer forms at the surface and grows towards the inside of the material.

Sectional photomicrographs of the specimens taken through a laser microscope were analyzed, and the average thickness l of the ferrite layer was determined according to Eq. (1).

$$l = \frac{A}{w} \quad (1)$$

Where w is the length of the layer along the boundary in the field of view, and A is the total area of the ferrite layer. **Figure 4** shows the relationship between l and the temperature of the isothermal annealing of the Fe-0.87 at% C alloy for 600 s to have the ferrite layer form. As seen here, in the annealing temperature range from 953 to 1153 K, l was 60 μm or more, but it fell to 10 μm or less when the annealing temperature was 1193 K.

As shown above, the thickness of the ferrite layer is larger when annealing is performed within the temperature range adequate for the formation of the ferrite layer than outside the range. The value of l increased with higher annealing temperature in the temperature range from 953 to 1073 K, and it decreased, in contrast, in the range of 1073 K or higher. The annealing temperature at which the ferrite layer grew thickest was 1073 K, where l was 170 μm . It was found in addition that l decreased markedly with the increase in annealing temperature in the range of 1153 K and higher. The growth of the ferrite layer in an Fe-1.1 at% C-0.22 at% Si-0.45 at% Mn alloy was studied through tests, and the growth rate of the layer was reported to be largest in a temperature range of 1073 to 1093 K.⁹⁾ This indicates that the temperature dependence of the ferrite layer growth of the above alloy is similar to that of the Fe-0.87 at% C alloy of the present study.

2.3 Rate-determining process of ferrite layer growth

Figure 5 shows sectional photomicrographs of the cold-rolled

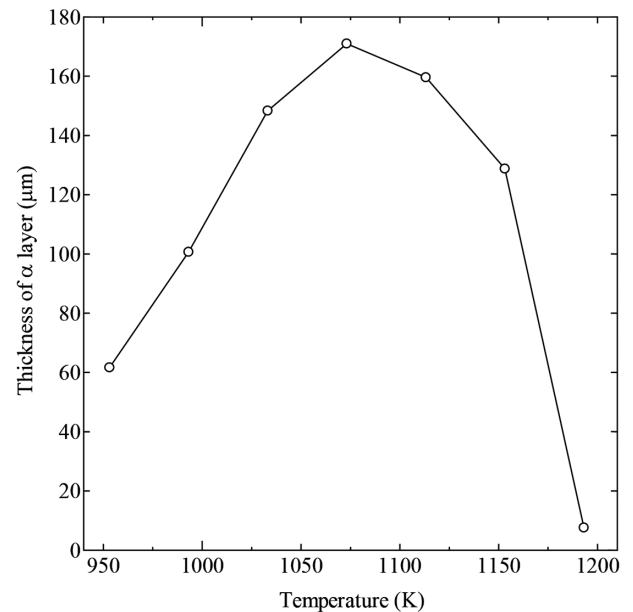


Fig. 4 Ferrite layer thickness versus annealing temperature of Fe-0.87 at% C alloy (annealing time 600 s)

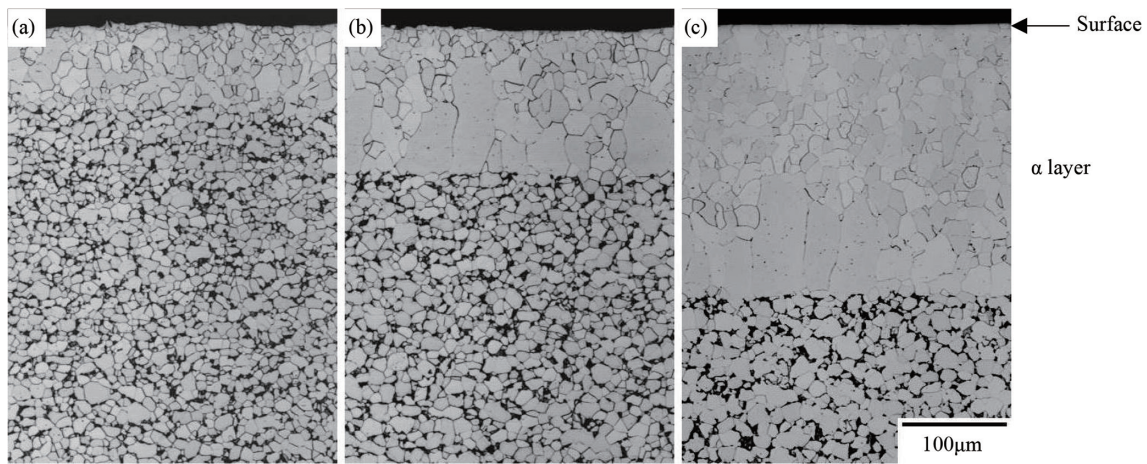


Fig. 5 Cross-sectional microstructures of Fe-0.87 at% C alloy annealed at 1073 K for (a) 100 s, (b) 400 s and (c) 1600 s

Fe-0.87 at% C alloy after isothermal annealing at 1073 K for periods from 100 to 1600 s; as stated earlier, 1073 K is the annealing temperature at which the ferrite layer growth was largest with the alloy. After any of the annealing periods, a ferrite layer formed at the specimen surface as in the case of annealing at 1033 K for 600 s, and the structure inside it consisted of α and P. It is clear from the comparison of these micrographs that, in addition to the growth of the ferrite layer thickness, α grains grew inside the layer with the annealing time at 1073 K. Coarse α grains appeared especially near the boundary between the ferrite layer and the inner structure of α and P.

According to the method for defining the average thickness of the ferrite layer described earlier, the value of l was calculated for different temperatures and periods of the annealing. Figure 6 shows the relationship between l and the time of isothermal annealing of the Fe-0.87 at% C alloy at 993, 1033, and 1073 K. Here, the ordinate represents l and the abscissa the annealing time, both in logarithms, and the points marked with circles correspond to the annealing temperature of 993 K, those with triangles to 1033 K, and those with squares to 1073 K. As is seen here, l increased monotonously with the increase in the annealing time at any of the annealing temperatures, and the plotting points for each annealing temperature were in a straight line.

Accordingly, allowing t to be the annealing time, l can be expressed in the form of an exponential function of t as given below:

$$l = k \left(\frac{t}{t_0} \right)^n \quad (2)$$

Where t_0 is a unit time, 1 s, and by dividing t by t_0 , the time term of the function is made dimensionless. The dimension of the proportionality factor k is the same as that of l , and n is dimensionless. The values of k and n were determined for each annealing temperature by analyzing the plotting points in Fig. 6 by the least-square method. The result was as follows: for 993 K, k was 4.54×10^{-6} m, and n was 0.49; for 1033 K, k was 5.19×10^{-6} m, and n was 0.52; and for 1073 K, k was 9.38×10^{-6} m, and n was 0.45. The value of n was near 0.5 for any of the annealing temperatures, which indicates that the parabolic rule applies to the relationship between l and t at any of the temperatures.

The ferrite layer growth following the parabolic rule points to the possibility of the rate of the growth being determined by the volume diffusion of atoms in the ferrite layer. On the other hand, at low temperature where atomic volume diffusion is limited, it is possible

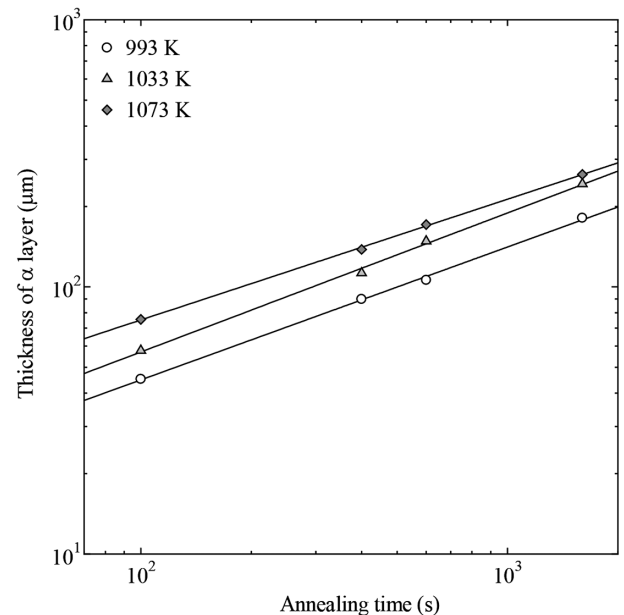


Fig. 6 Ferrite layer thickness versus annealing time of Fe-0.87 at% C alloy at 993, 1033 and 1073 K

that the grain-boundary diffusion of atoms significantly contributes to the ferrite layer growth. When the grains in the ferrite layer grow under such a condition, the ratio of grain boundaries in the ferrite layer decreases with the annealing time, and since this decrease in the ratio lowers the contribution of the grain-boundary diffusion to the ferrite layer growth, n falls to less than 0.5. If there is little growth of the grains in the ferrite layer, however, the ratio of grain boundaries in the ferrite layer remains substantially unchanged during isothermal annealing, and in this case, n is equal to 0.5. It follows, therefore, that when n is equal to 0.5, namely the parabolic rule applies to the relationship between l and t , two possibilities have to be considered about the rate-determining process.^{24, 25)}

To identify the rate-determining process for the ferrite layer growth, we analyzed the grain growth behavior in the ferrite layer. The metallographic structures in the sectional micrographs were analyzed using the quadrature method described earlier,²²⁾ and the average diameter d of α grains in the ferrite layer was calculated. Figure 7 shows the relationship between d and the time of isothermally

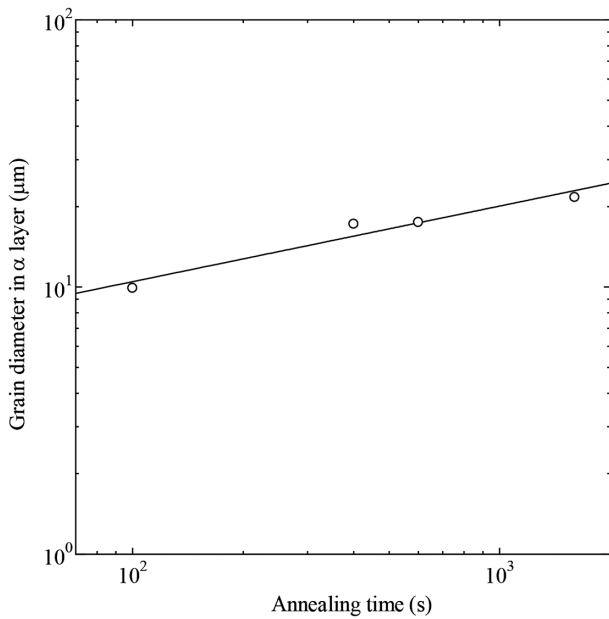


Fig. 7 Grain size of ferrite layer versus annealing time at 1073 K

annealing the Fe-0.87 at% C alloy at 1073 K. Here, the ordinate represents d and the abscissa the annealing time, both in logarithms. As the graph shows, d increased monotonously with the annealing time, and the plotted points nearly aligned along a straight line. Allowing t to be the annealing time, therefore, d is expressed in the form of an exponential function of t as given below.²⁵⁾

$$d = k_d \left(\frac{t}{t_0} \right)^m \quad (3)$$

Where t_0 is a unit time, 1 s, and in the same way as with Eq. (2), by dividing t by t_0 , the time term of the function is made dimensionless. The dimension of the proportionality factor k_d is the same as that of d , and m is dimensionless. By analyzing the plotting points in Fig. 7, the value of k_d was calculated at 2.84×10^{-6} m, and that of m at 0.28.

When the rate of the ferrite layer growth is assumed to be determined by the grain-boundary diffusion of atoms in it, the relationship between n and m satisfies Eq. (4).^{24, 25)}

$$n = \frac{1-m}{2} \quad (4)$$

Assuming $m=0.28$, n is equal to 0.36 from Eq. (4). As stated earlier, however, n is close to 0.5 when the annealing temperature is 1073 K. This indicates that the rate of the ferrite layer growth is not determined by the grain-boundary diffusion of atoms but by their volume diffusion.

2.4 Prediction of ferrite layer through decarburization

Figure 8 is the phase diagram of the Fe-cementite system in the Fe-C binary system according to Gustafson's calculation.²⁶⁾ This was drawn up using Thermo-Calc ver. 4.1 and based on the thermodynamic databases for α , γ , and θ of TCFE6.²⁷⁾ The ordinate represents temperature in K and the abscissa carbon concentration in at%. The curves $c_{\alpha\gamma}$, $c_{\gamma\alpha}$, $c_{\alpha\theta}$, and $c_{\gamma\theta}$ show the phase-interface compositions $a/(\alpha+\gamma)$, $\gamma/(\alpha+\gamma)$, $a/(\alpha+\theta)$, and $\gamma/(\gamma+\theta)$, respectively. The dotted line represents the C concentration of the Fe-0.87 at% C alloy, which is referred to as c_0 . As shown here, the temperature T_3 of A_3 transformation ($\gamma \leftrightarrow \alpha$) is 1185 K, and the temperature T_e of eutectoid transformation ($\gamma \leftrightarrow \alpha+\theta$) is 1000 K. The A_{e3} temperature of the Fe-0.87 at% C alloy is 1113 K.

When this alloy is isothermally annealed at 1113 K or lower, a

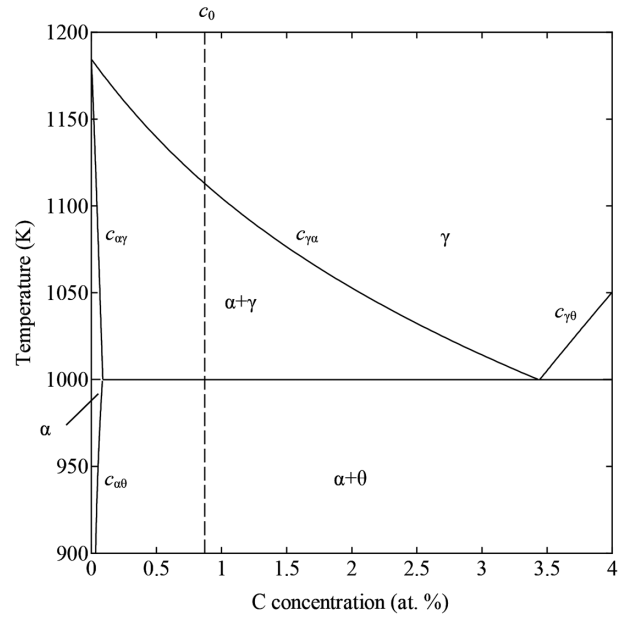


Fig. 8 Calculated phase diagram of Fe-C binary system

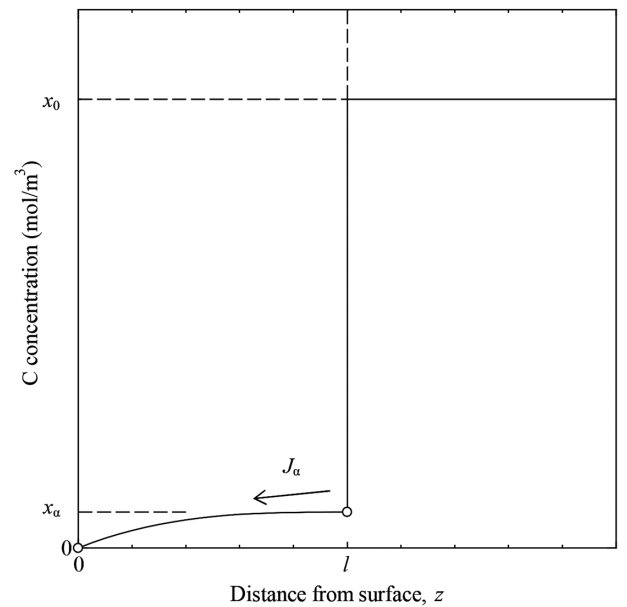


Fig. 9 Schematic profile of C concentration in surface ferrite layer and inside dual-phase structure of ferrite and austenite

dual phase of $\alpha+\theta$ forms at a temperature lower than T_e , and another of $\alpha+\gamma$ at a temperature higher than the same. The carbon concentration profile in the direction perpendicular to the sheet surface is considered regarding specimens isothermally annealed for a prescribed time t at the temperature at which a dual phase microstructure of $\alpha+\gamma$ forms.²⁸⁾ A ferrite layer of an even thickness forms at the surface when the carbon concentration at the surface falls to $c_{\alpha\gamma}$ or less owing to decarburizing. Figure 9 shows a schematic profile of carbon concentration in this case. The ordinate represents the mol concentration of carbon, and the abscissa the distance from the surface; the mol concentration is the quotient of the molar fraction of the element in question divided by its molar volume, and its unit is mol/m³. The molar volume of α at 1184 K is 7.37×10^{-6} m³/mol, and

that of γ is $7.30 \times 10^{-6} \text{ m}^3/\text{mol}$.²⁹⁾

In the graph, x_0 is the mol concentration of C in the Fe-0.87 at% C alloy, carbon concentration at the surface is assumed to be 0, and x_α is the mol concentration of C on the ferrite-layer side ($z=l$) of the boundary between the ferrite layer and the dual phase of $\alpha+\gamma$. When it is assumed that the rate of the ferrite layer growth is defined by the volume diffusion of C atoms, a local equilibrium is presumed there to be at the boundary, and in this case, x_α corresponds to $c_{\alpha\gamma}$ in Fig. 8. In addition, since the mol concentration of C on the $\alpha+\gamma$ dual-phase side ($z=l_+$) of the boundary is x_0 , the boundary conditions are expressed by the equations given below.

$$x(z=0, t>0) = 0 \quad (5a)$$

$$x(z=l_-, t>0) = x_\alpha \quad (5b)$$

$$x(z \geq l_+, t>0) = x_0 \quad (5c)$$

The boundary shifts and the ferrite layer grows while satisfying these boundary conditions. Because the driving force of the boundary shift is the difference in the flux of C diffusion on the two sides of the boundary, the rate v of the boundary shift is expressed by Eq. (6).

$$(x_0 - x_\alpha)v = J_\alpha \quad (6)$$

Where J_α is the flux of C diffusion on the ferrite-layer side of the boundary; according to Fick's first law, it changes in proportion to the gradient of the C concentration in the ferrite layer, and is expressed by Eq. (7) given below.

$$J_\alpha = -D_\alpha \left(\frac{\partial x}{\partial z} \right) \quad (7)$$

Here, D_α is the volume diffusion coefficient of C in α . The C concentration profile in the ferrite layer follows Fick's second law, which is expressed as Eq. (8) when D_α does not change depending on C concentration.

$$\frac{\partial x}{\partial t} = D_\alpha \frac{\partial^2 x}{\partial z^2} \quad (8)$$

When a local equilibrium is maintained at the layer boundary in the isothermal transformation of a binary alloy, l is expressed as a function of t as in Eq. (9).²⁸⁾

$$l = 2\beta\sqrt{D_\alpha t} \quad (9)$$

Here, β is a growth rate constant, dimensionless. The nonlinear equation of β expressed by Eq. (10) is obtained by solving Eq. (8) using Eq. (9) under the conditions of Eqs. (5a) and (5b) of the boundary conditions described earlier.^{6, 28)}

$$\sqrt{\pi}\beta \exp(-\beta^2) \operatorname{erf}(\beta) = \frac{x_\alpha}{x_0 - x_\alpha} \quad (10)$$

When x_0 and x_α are known, β at temperature T is obtained by numerical calculation, and the position of the boundary, or the thickness of the ferrite layer l , at time t is obtained. Note that l at the temperature at which the $\alpha+\theta$ dual phase forms can be obtained likewise by the above analysis. In this case, x_α corresponds to the phase interface $c_{\alpha\theta}$ between the α phase and the $\alpha+\theta$ phase.

On the other hand, when the Fe-0.87 at% C alloy is isothermally annealed at 1113 K or higher, a single-phase structure of γ forms. Then, with respect to the specimens isothermally annealed for a time t at the temperature at which a single-phase γ structure forms, the C concentration profile in the direction perpendicular to the surface is examined. When the C concentration at the surface falls to $c_{\alpha\gamma}$ or less as a result of decarburization at 1185 K or lower, a ferrite layer of an even thickness l forms at the surface. **Figure 10** shows a schematic profile of the C concentration in this case. To study the growth rate of the layer under this condition, it is necessary to consider the C diffusion flux J_γ in the γ structure on the inner side of the boundary in addition to the C diffusion flux J_α on its ferrite side. The

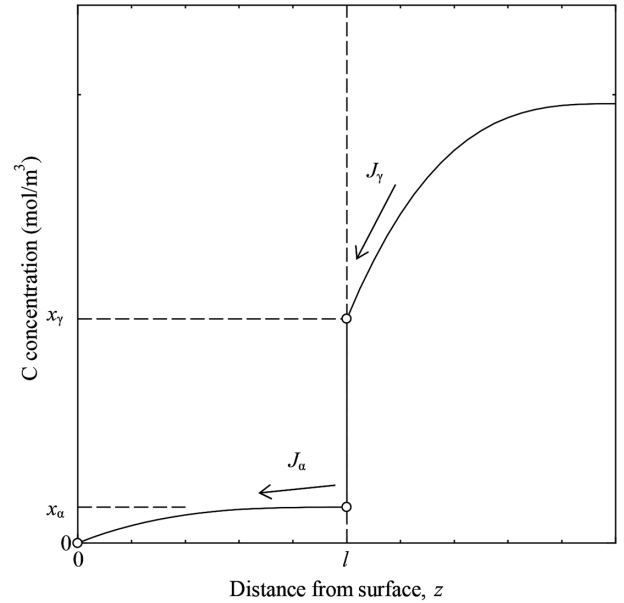


Fig. 10 Schematic profile of C concentration in surface ferrite layer and inside single-phase structure of austenite

mol concentration of C x_γ on the inner side of the boundary corresponds to the interface curve $c_{\alpha\gamma}$ between the γ and the $\alpha+\gamma$ phases. For this reason, the growth rate constant β in the temperature range from 1113 to 1185 K satisfies a nonlinear equation not of Eq. (10) but Eq. (11).

$$\sqrt{\pi} = \frac{x_\alpha}{(x_\gamma - x_\alpha)\beta \exp(\beta^2) \operatorname{erf}(\beta)} + \frac{x_\gamma - x_0}{(x_\gamma - x_\alpha)\beta \exp\left(\beta^2 \frac{D_\alpha}{D_\gamma}\right) \left\{ 1 - \operatorname{erf}\left(\beta \sqrt{\frac{D_\alpha}{D_\gamma}}\right) \right\}} \sqrt{\frac{D_\gamma}{D_\alpha}} \quad (11)$$

Where D_γ is the volume diffusion coefficient of C in γ .

When both sides of Eq. (9) are squared, Eq. (12) is obtained, which demonstrates that the parabolic rule applies to the relationship between l and t .

$$l^2 = 4\beta^2 D_\alpha t = Kt \quad (12)$$

Where K is the parabolic coefficient, and its unit is m^2/s , the same as that of the diffusion coefficient. It is an important parameter expressing the growth rate of the ferrite layer.

Then, studies of the temperature dependence of K of the Fe-0.87 at% C alloy are presented below under the assumption that α and γ are equal in terms of molar volume. Based on the thermodynamic databases of TCFE6, the phase interface curves $\alpha/(\alpha+\gamma)$, $\gamma/(\alpha+\gamma)$, and $\alpha/(\alpha+\theta)$ were calculated using Thermo-Calc ver. 4.1 as explained earlier.²⁷⁾ Both D_α and D_γ were expressed as Eqs. (13) and (14), respectively, based on values in published literatures.^{30, 31)}

$$D_\alpha = 2 \times 10^{-6} \exp\left(-\frac{10115}{T}\right) \cdot \exp\left\{0.5898 \left[1 + \frac{2}{\pi} \arctan\left(\frac{15629}{1043} - \frac{15309}{T}\right) \right] \right\} \quad (13)$$

$$D_\gamma = 4.53 \times 10^{-7} \left\{ 1 + u_c(1-u_c) \frac{8339.9}{T} \right\} \cdot \exp\left[-\left(\frac{1}{T} - 2.221 \times 10^{-4} \right) (17767 - 26436u_c) \right] \quad (14)$$

Here, the unit of D_α and D_γ is m^2/s , that of T is K, and u_c is the u-fraction of C. According to Eq. (14), D_γ changes depending on C

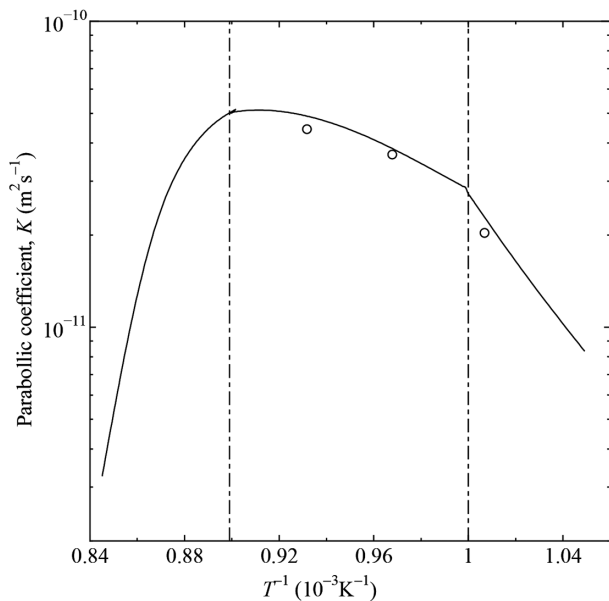


Fig. 11 Parabolic coefficient of Fe-0.87 at% C alloy versus annealing temperature

concentration, and in consideration of this, D_γ is approximated as Eq. (15) below:³²⁾

$$D_\gamma = \frac{\int_{C_0}^{C_\gamma} D_\gamma dx}{C_\gamma - C_0} \quad (15)$$

Figure 11 shows the relationship between the parabolic coefficient K and temperature T ; here, the ordinate represents the logarithm of K , the abscissa the inverse of T , and the curve shows the relationship predicted based on the model of the ferrite layer growth rate determined by C diffusion (moving boundary model) described earlier. The graph shows that K is largest at the temperature at which the $\alpha+\gamma$ dual-phase forms. In addition, at 1113 K ($A_{\alpha\gamma}$) or higher, K decreases rapidly with increasing T .¹³⁾ This prediction agrees quantitatively with the structural observation shown in Fig. 2 and the ferrite layer thickness measurement shown in Fig. 4. In addition, based on an analysis of the ferrite layer growth at different temperatures shown in Fig. 6, the value of K is 2.0×10^{-11} m²/s at 993 K, 3.6×10^{-11} m²/s at 1033 K, and 4.4×10^{-11} m²/s at 1073 K; these results are plotted in the graph with open circles. The values of K actually measured in the isothermal annealing test were close to the predicted ones. It is possible to conclude, therefore, that when the Fe-0.87 at% C alloy is isothermally held at 993 to 1073 K for 100 to 1600 s, the ferrite layer forming at the surface grows at a rate determined by the volume diffusion of C atoms.

3. Conclusion

To clarify the rate-determining process for the decarburizing reaction of an Fe-0.87 at% C alloy, we investigated the growth of the ferrite layer forming at the surface during isothermal annealing and the grain growth in the layer. The structure that forms through isothermal annealing at 953 K proved to be a dual-phase structure of ferrite and cementite, a dual-phase structure of ferrite and austenite

when the annealing temperature was from 993 to 1073 K, and a single-phase austenite structure when the temperature was 1153 K or higher. Different from the above structure in the inside, however, a ferrite layer forms at the surface as a result of decarburizing at 1153 K or lower; the ferrite layer formation is predictable from the calculated phase diagram for the Fe-C binary system. The relationship between the average thickness of the surface ferrite layer and the annealing time follows the parabolic rule. In addition, the grains in the ferrite layer were found to grow larger with the annealing time. This indicates that the growth rate of the ferrite layer is determined by the volume diffusion of atoms. The parabolic coefficient of the ferrite layer growth was calculated using a moving boundary model taking into consideration the growth rate being determined by the volume diffusion of C atoms in the ferrite layer, and the values thus obtained substantially agreed with the parabolic constant obtained through measurement in the isothermal annealing test.

References

- 1) Leslie, W.C.: The Physical Metallurgy of Steels. McGraw-Hill, New York, 1981, p. 211
- 2) Birks, N., Meier, G.H., Pettit, F.S.: High-Temperature Oxidation of Metals. Second Edition. Cambridge University Press, 2006, p. 151
- 3) Hankins, G.A., Becker, M.L.: J. Iron Steel Inst. 124, 387 (1931)
- 4) Kawase, H., Yoshida, K., Nakagawa, T.: Nisshin Steel Tech. Rep. 31, 15 (1973)
- 5) Owaku, S.: Netsusyori. 36, 388 (1996)
- 6) Smith, R.P.: Trans. TMS-AIME. 224, 105 (1962)
- 7) Phillion, A., Zurob, H.S., Hutchinson, C.R., Guo, H., Malakhov, D.V., Nakano, J., Purdy, G.R.: Metall. Trans. A. 35A, 1237 (2004)
- 8) Zurob, H.Z., Hutchinson, C.R., Beche, A., Purdy, G.R., Brechet, Y.: Acta Mater. 56, 2203 (2008)
- 9) Naito, I.: Tetsu-to-Hagané. 22, 17 (1936)
- 10) Naito, I.: J. Jpn. Inst. Met. 5, 25 (1941)
- 11) Pennington, W.A.: Trans. Am. Soc. Met. 37, 48 (1946)
- 12) Oikawa, H., Remy, J.F., Guy, A.G.: Trans. ASM. 61, 110 (1968)
- 13) Kajihara, M.: Mater. Trans. 53, 1896 (2012)
- 14) Tonomura, K., Higo, Y.: Nisshin Steel Tech. Rep. 27, 32 (1972)
- 15) Pyyry, I., Kettunen, P.: Scand. J. Metall. 2, 265 (1973)
- 16) Marder, A.R., Perpetua, S.M., Kowalik, J.A., Stephenson, E.T.: Metall. Trans. A. 16A, 1160 (1985)
- 17) Nomura, M., Morimoto, H., Toyama, M.: ISIJ Int. 40, 619 (2000)
- 18) Shewmon, P.G.: Transformations in Metals. McGraw-Hill, New York, 1969, p. 63
- 19) Yamada, T., Miura, K., Kajihara, M., Kurokawa, N., Sakamoto, K.: Mat. Sci. Eng. A. 390, 118 (2005)
- 20) Tanaka, Y., Kajihara, M., Watanabe, Y.: Mat. Sci. Eng. A. 445-446, 355 (2007)
- 21) Oldani, C.R.: Scr. Mater. 35, 1253 (1996)
- 22) Umamoto, M.: Bull. Iron Steel Inst. Jpn. 2, 731 (1997)
- 23) Birks, N., Jackson, W.: J. Iron Steel Inst. 208, 81 (1970)
- 24) Corcoran, Y.L., King, A.H., de Lanerolle, N., Kim, B.: J. Electron. Mater. 19, 1177 (1990)
- 25) Furuto, A., Kajihara, M.: Mater. Trans. 49, 294 (2008)
- 26) Gustafson, P.: Scan. J. Metall. 14, 259 (1985)
- 27) Thermo-Calc software AB: TCS Steel and Fe-Alloys Database Version 6.2. Thermo-Calc Software, 2006
- 28) Wagner, C., Jost, W.: Diffusion in Solids, Liquids and Gases. Academic Press, New York, 1960, p. 69
- 29) Kajihara, M.: J. Mater. Sci. 44, 2109 (2009)
- 30) Agren, J.: Acta Metall. 30, 841 (1982)
- 31) Agren, J.: Scr. Metall. 20, 1507 (1986)
- 32) Trivedi, R., Pound, M.C.: J. Appl. Phys. 38, 3569 (1967)

NIPPON STEEL & SUMITOMO METAL TECHNICAL REPORT No. 120 DECEMBER 2018



Koutarou HAYASHI
Senior Researcher, PhD in Engineering
Sheet & Coil Research Lab.
Steel Research Laboratories
20-1 Shintomi, Futtsu City, Chiba Pref. 293-8511



Toshinobu NISHIBATA
Senior Researcher
Fundamental Metallurgy Research Lab.
Advanced Technology Research Laboratories